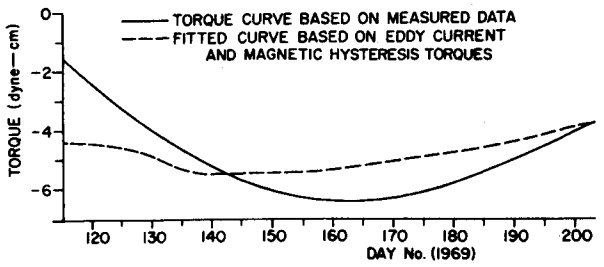

Fig. 4 Fitted torque curve.

symmetric with respect to the satellite mass center, causes the net bombardment of charged ions of the ionosphere to impact with an unsymmetrical distribution, therefore, causing a torque; 2) torque from $\mathbf{V} \times \mathbf{B}$ induced current (induction torque)[11]—a $\mathbf{V} \times \mathbf{B}$ induced potential across the dipole antenna results in a flow of electrons along the antenna,[14] which in turn interacts with the Earth's magnetic field to produce an electrostatic force and consequently a torque. The $\mathbf{V} \times \mathbf{B}$ potential distribution is dependent on photoemission,[11,14] and consequently the resulting torques have a dependence on percent sun (Fig. 1).

Several combinations of the previously discussed torques may be conjectured as the cause of the anomalous measured torque history. The quality and amount of measured dynamics data on ISIS-I does not permit the various mechanisms to be isolated and conclusively identified at this point.

References

[1] Paghis, I., Franklin, C. A., and Mar, J., "Alouette I, The First Three Years in Orbit," DRTE Rept. 1169, March 1967, Dept. of National Defence, Ottawa, Canada.

[2] Etkin, B. and Hughes, P. C., "Explanation of the Anomalous Spin Behavior of Satellites with Long Flexible Antennas," *Journal of Spacecraft and Rockets*, Vol. 4, No. 9, Sept. 1967, pp. 1139–1145.

[3] Mar, J. and Garrett, T., "Mechanical Design and Dynamics of the Alouette Spacecraft" *Proceedings of the IEEE*, Vol. 57, No. 6, June 1969, pp. 882–896.

[4] Hughes, P. C. and Cherchas, D. B., "Spin Decay of Explorer XX," *Journal of Spacecraft and Rockets*, Vol. 7, No. 1, Jan. 1970, pp. 92–93.

[5] Florida, C. D., "The ISIS Series of Ionospheric Satellites," *Proceedings of the Eighth International Symposium on Space Technology and Science*, Tokyo, 1969, AGNE Publishing, Japan, pp. 1073–1087.

[6] Kowalik, H., "A Spin and Attitude Control System for the ISIS-I and ISIS-B Satellites," *Automatica*, Vol. 6, 1970, pp. 673–682.

[7] Vigneron, F. R. and Garrett, T. W., "Solar Induced Distortion—Atmospheric Drag Coupling in Alouette Satellites," DRTE Rept. 1171, Feb. 1967, Dept. of National Defence, Ottawa, Canada.

[8] Wilson, R. A., "Rotational Magnetodynamics and Steering of Space Vehicles," TN D-566, Sept. 1961, NASA.

[9] Fischell, R. E., "Magnetic Damping of the Angular Motions of Earth Satellites," *American Rocket Society Journal*, Vol. 31, No. 9, Sept. 1961, pp. 911–913.

[10] Yu, Y. E., "Spin Decay, Spin-Precession Damping, and Spin Axis Drift of the Telestar Satellite," *Bell System Technical Journal*, Vol. 42, Sept. 1963, pp. 2169–2193.

[11] Wood, G. P. and Hohl, F., "Electric Potentials, Forces, and Torques on Bodies Moving Through Rarefied Plasmas," *Proceedings of the AIAA and Northwestern University 6th Biennial Gas Dynamics Symposium*, Evanston, Ill., Aug. 25–27, 1965.

[12] Hohl, F. and Wood, G. P., "The Electrostatic and Electromagnetic Drag Forces on a Spherical Satellite in a Rarefied, Partially Ionized Atmosphere," *Rarefied Gas Dynamics*, Academic Press, New York, 1963, pp. 45–64.

[13] Brundlin, C. L., "Effects of Charged Particles on the Motion of an Earth Satellite," *AIAA Journal*, Vol. 1, No. 11, Nov. 1963, pp. 2529–2538.

[14] Kasha, M., *The Ionosphere and Its Interaction With Satellites*, Gordon and Breach, New York, 1969, Chap. 5.

Injection into a Supersonic Stream from the Windward Side of Sweptback Injectors at Angle of Attack

M. Hersch* and L. A. Povinelli†

NASA Lewis Research Center, Cleveland, Ohio

It has previously been shown[1–3] that vortices, generated by delta wing injectors at an angle of attack, can enhance penetration and mixing of a secondary jet into a supersonic stream. In these previous studies helium was injected at sonic velocity normal to the leeward side of the injectors directly into the vortex region. Although penetration and mixing were improved in comparison to injection from a flat plate in a vortex free flowfield, two problems were noted. Firstly, a significant portion of the jet was not captured by the vortex, but flowed directly downstream as if injected from a flat plate in a vortex free flowfield.[2] Secondly, the jet appeared to disrupt the vortex motion.[3] These problems might be overcome by matching the direction and velocity of the jet to the vortex.

An alternate injection technique is suggested by the fact that the leeward vortex originates from flow which sweeps over the leading edge from the windward side of the wing.[4] It might be anticipated then, that injectant from the windward side would be carried by this flow into the leeward vortex. Also, disruption of the vortex might be minimized if the injectant were introduced at a low velocity distributed over a large area. This might be accomplished by injecting the gas from a porous surface as opposed to discrete orifices. In this study two injectors were tested to explore these ideas (Figs. 1 and 2).

One injector, configuration A (Fig. 1), had a single sharp leading edge sweptback at 58.5°. This injector may be

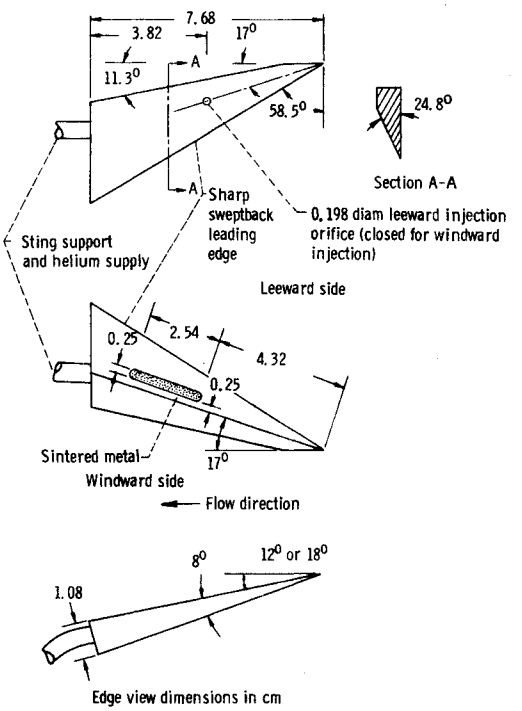

Fig. 1 Injector configuration A.

Received June 24, 1971.

* Aerospace Research Scientist, Hypersonic Propulsion Section.

† Aerospace Research Scientist, Hypersonic Propulsion Section. Associate Fellow AIAA.

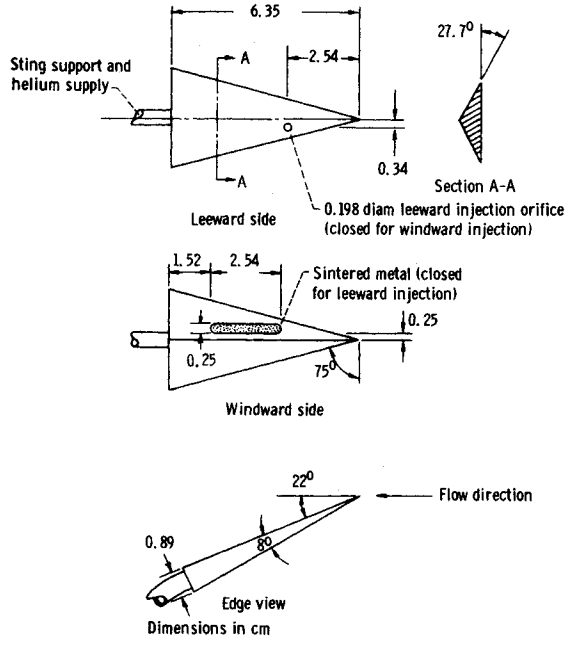

Fig. 2 Symmetrical full delta injector. Configuration B.

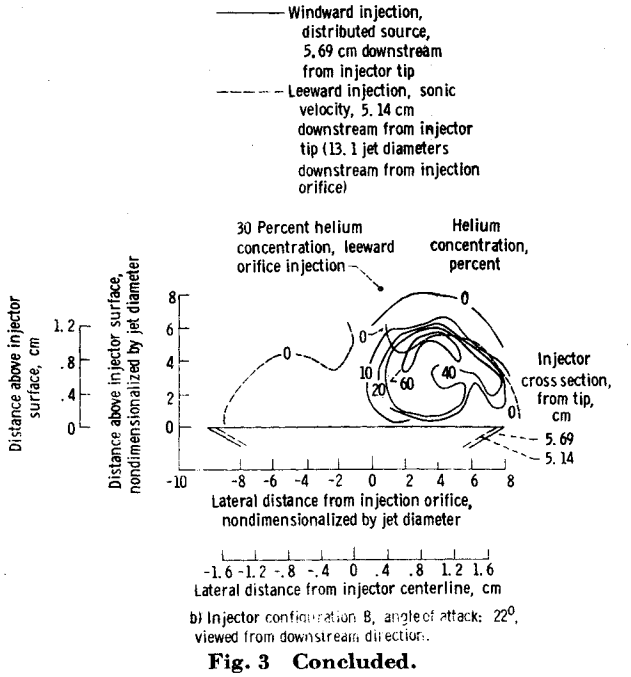

Fig. 3 Concluded.

considered to be one-half of an arrow wing if a line through the apex is taken to be a line of symmetry. The other injector, configuration B (Fig. 2), was a delta wing with sweepback angles of 75°.

Helium was injected from a porous sintered metal surface on the windward side, or at sonic velocity from a 0.198 cm orifice on the leeward side of the injectors. The porosity of the sintered metal was approximately 44%. Total injection pressure was 3.45×10^5 N/m^2 (50 psia). Injectant mass flow was constant for all tests. Freestream velocity and total pressure were Mach 2, and 9.58×10^4 N/m^2 (13.9 psia), respectively. Wind-tunnel dimensions were 9.75 by 25.4 cm. Helium penetration and distribution were determined by withdrawing gas from the freestream and measuring the helium content with a mass spectrometer. The sampling and analysis technique have previously been described.[1]

Helium distribution resulting from leeward and windward injection for the two configurations is shown in Fig. 3. Configuration A was mounted at 12° angle of attack for leeward injection and 12° or 18° for windward injection. Configuration B was mounted at 22° angle of attack for both modes of injection.

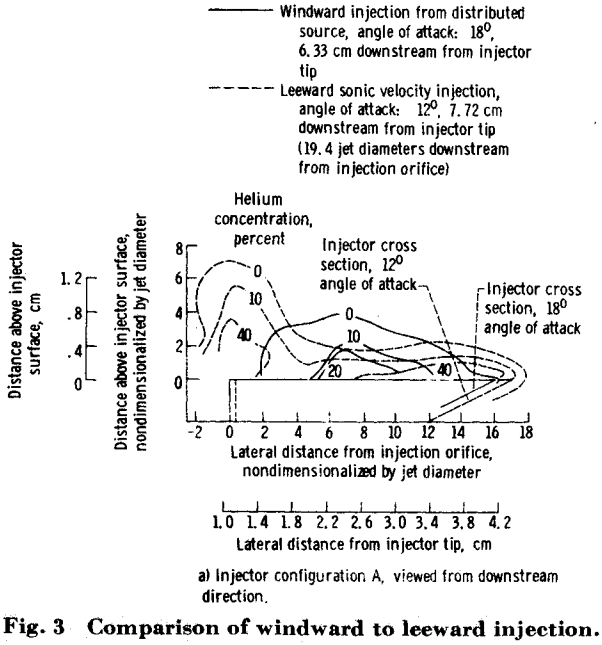

Fig. 3 Comparison of windward to leeward injection.

In all cases of leeward injection, a large portion of the helium flowed directly downstream from the orifice and was not captured by vortex. This is indicated by the high humps in the leeward distribution patterns shown in Fig. 3a and b. The maximum extent of the helium region directly downstream of the leeward orifice was not established though for the symmetrical delta wing injector (Fig. 3b). However, in this region helium concentration was 30% at approximately 7.5 jet diameters above the injector surface as shown in Fig. 3b. As previously shown,[1-3] this portion of the helium behaves as if it were injected from a flat plate in a vortex free flowfield.

With windward injection using configurations A and B mounted at 18° and 22° angle of attack, respectively, helium was carried over the swept edge and captured by the leeward vortex. No helium was detected over the leeward side of configuration A at 12° angle of attack using windward injection. This indicates that a minimum angle of attack is needed for helium to be carried from the windward to leeward regions. The minimum angle of attack, though not determined here, was evidently between 12° and 18° for configuration A.

As shown in Fig. 3a and b, at any particular lateral position across the injector, helium penetration may be greater for one injection technique than another. It is, therefore, difficult to draw general quantitative conclusions concerning penetration and spreading from these measurements. These results do show, however, that a significant portion of the helium, when injected from the orifice on the leeward surface, is not captured by the vortex but flows directly downstream as if injected from a flat plate. The vortex is, therefore, not efficiently utilized in aiding penetration and mixing of the injectant with the freestream. In contrast, helium, when injected from a porous source on the windward surface was carried over the swept edge and completely filled the vortex region. The results of Fig. 3b indicate that both leeward vortex regions would have been filled with helium had porous injection strips been located on both, rather than only one of the windward surfaces.

Windward injection might be a useful injector cooling technique. Aerodynamic heating of a swept injector at an

angle of attack is greatest on the swept edges and windward surface. The results of this study show that these areas can be sheathed by a layer of cool gas supplied by windward injection.

References

[1] Povinelli, L. A., Povinelli, F. P., and Hersch, M., "A Study of Helium Penetration and Spreading in a Mach 2 Airstream Using a Delta Wing Injector," TN D-5322, 1969, NASA.

[2] Povinelli, F. P., Povinelli, L. A., and Hersch, M., "Effect of Angle of Attack and Injection Pressure on Jet Penetration and Spreading From a Delta Wing in Supersonic Flow," TM X-1889, 1969, NASA.

[3] Hersch, M. and Povinelli, L. A., "Effect of Interacting Vortices on Jet Penetration into a Supersonic Stream," TM X-2134, 1970, NASA.

[4] Roy, M., "Vortices from the Apex and Sheets in Cornet," *Recherche Aeronautique*, No. 56, Feb. 1957; also *On the Theory of the Delta Wing*, edited by M. H. Snyder, AR-66-4, CR-81254, Sept. 1966, NASA, pp. 11–40.

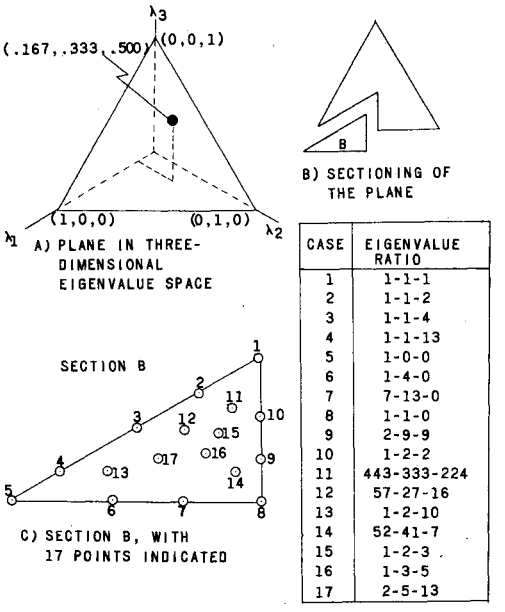

CASE	EIGENVALUE RATIO
1	1-1-1
2	1-1-2
3	1-1-4
4	1-1-13
5	1-0-0
6	1-4-0
7	7-13-0
8	1-1-0
9	2-9-9
10	1-2-2
11	443-333-224
12	57-27-16
13	1-2-10
14	52-41-7
15	1-2-3
16	1-3-5
17	2-5-13

Fig. 1 Definition of eigenvalue ratios.

A New Guidance System Figure-of-Merit

GEORGE R. YOUNG*

NASA Langley Research Center, Hampton, Va.

A CONVENIENT parameter to determine the relative effectiveness of a launch vehicle in delivering a spacecraft onto an interplanetary trajectory and to determine midcourse velocity budgets is the expected value of the midcoursec orrection velocity magnitude v. The parameter in common use, while it is sometimes called the expected value of v, is the square root of the trace of the midcourse velocity covariance matrix.[1]

The figure-of-merit, defined in this manner, is often used to approximate midcourse correction velocity budgets by using the further approximation[2]

$$\mu|\bar{v}| + 3\sigma|\bar{v}| \simeq 3\text{FOM} \tag{1}$$

where $|\bar{v}| = v = (v_1^2 + v_2^2 + v_3^2)^{1/2}$, $\mu|\bar{v}|$ is the mean of v, and $\sigma|\bar{v}|$ is the standard deviation of v.

This approximation is equivalent to assuming that the mean magnitude is zero (which would be true for a linear process with the means of the components zero) and, therefore, that the second moment of the magnitude about zero is the standard deviation.

Using Eq. (1) the probability that v does not exceed 3FOM is greater than or equal to 99%

$$P[v \leq 3\text{FOM}] \geq 0.99 \tag{2}$$

where v_1,v_2,v_3 = components of $\bar{v}$ in any Cartesian coordinate system.

It is the purpose of this Note to suggest a new FOM, for which Eq. (2) is still true, that saves between 13 and 30% of the v budget. The new approximation has one other, important, characteristic. It distinguishes between two midcourse velocity matrices with the same trace but with different midcourse velocity requirements. Since the old FOM is used extensively to compare the midcourse requirements for different trajectories, this is a serious deficiency that can be eliminated by the new approximation.

This new FOM is based on an analysis by Hoffman and Young[3] who obtained an approximation to the mean and variance of v by expanding v^n in a Taylor series about a point in a transformed space defined by

$$v_1^* = |v_1|, \qquad v_2^* = |v_2|, \qquad v_3^* = |v_3| \tag{3}$$

truncating after the second-order terms and integrating over the transformed density function to define the nth moment of v. The components v_1, v_2, and v_3 were assumed to be normally distributed with mean zero. The analysis resulted in the approximations

$$\mu|\bar{v}| = E(|\bar{v}|) \simeq (2T/\pi)^{1/2}[1 + (\pi - 2)\beta/(2A)^{1/2}T^2] \tag{4a}$$

$$\sigma|\bar{v}|^2 \simeq T - \{(2T/\pi)^{1/2}[1 + (\pi - 2)\beta/(2A)^{1/2}T^2]\}^2 \tag{4b}$$

where $\lambda_1,\lambda_2,\lambda_3$ = eigenvalues of the v matrix, T = trace of the v matrix = $\lambda_1 + \lambda_2 + \lambda_3$, $|\bar{v}|$ = magnitude of the v vector $(v_1,v_2,v)^T$, A = constant used to find the best point about which to expand, $E[\ ]$ = expected value operator, and $\beta = \lambda_1\lambda_2 + \lambda_1\lambda_3 + \lambda_2\lambda_3$. The series expansion was made about the point $[(A\lambda_1/\pi)^{1/2},(A\lambda_2/\pi)^{1/2},(A\lambda_3/\pi)^{1/2}]$. The maximum percentage error in the variance of v was minimized resulting in a value of 2.7 for A.

The new FOM is taken to be

$$\text{FOM} = \mu|\bar{v}| + 3\sigma|\bar{v}| \tag{5}$$

with the mean given by Eq. (4a) and the standard deviation by Eq. (4b). To check the accuracy for this new FOM 17 covariance matrices were chosen to be representative of general midcourse correction covariance matrices. Each of the matrices was chosen such that $T = 1$ and the eigenvalues had the various ratios defined in Fig. 1.

In Fig. 1a is presented a plane in three-dimensional eigenvalue space equivalent to $T = 1$. Every choice of three eigenvalues (with $T = 1$) must be a point on the plane. In Fig. 1b is a small sketch indicating that the eigenvalue plane has been sectioned, and Sec. B is presented in Fig. 1c. The 17 points are indicated along with the corresponding eigenvalue ratios. Because of symmetry of the mathematical formulation, each point of Sec. B is equivalent to a point on each of the remaining five sections. Investigating the results for these 17 cases is equivalent to considering 76 points in the eigenvalue plane which should be more than adequate.

Received May 14, 1971; revision received July 9, 1971.

Navigation, Control, and Guidance Theory; Spacecraft Mission Studies and Economics; Lunar and Planetary Trajectories.

* Head, Mission Applications Section, Mission Analysis and Applications Branch, Space Technology Division.